Article

Powders Synthesized from Calcium Carbonate and Water Solutions of Potassium Hydrosulfate of Various Concentrations

Tatiana V. Safronova *, Peter D. Laptin, Alexandra I. Zybina, Xiaoling Liao, Tatiana B. Shatalova, Olga V. Boytsova, Dinara R. Khayrutdinova, Marat M. Akhmedov, Zichen Xu, Muslim R. Akhmedov

Posted Date: 22 August 2024

doi: 10.20944/preprints202408.1485.v1

Keywords: potassium hydrosulfate; calcium carbonate; heterophase synthesis; syngenite; gypsum; arcanite

Preprints.org (www.preprints.org) | NOT PEER-REVIEWED | Posted: 22 August 2024 doi:10.20944/preprints202408.1485.v1

Article

Powders Synthesized from Calcium Carbonate and Water Solutions of Potassium Hydrosulfate of Various Concentrations

Tatiana V. Safronova [1,2,*], Peter D. Laptin [2], Alexandra I. Zybina [2], Xiaoling Liao [3], Tatiana B. Shatalova [1,2], Olga V. Boytsova [1,2], Dinara R. Khayrutdinova [4], Marat M. Akhmedov [5], Zichen Xu [3] and Muslim R. Akhmedov [6]

[1] Department of Chemistry, Lomonosov Moscow State University, Building, 3, Leninskie Gory, 1, 119991 Moscow, Russia
[2] Department of Materials Science, Lomonosov Moscow State University, Building, 73, Leninskie Gory, 1, 119991 Moscow, Russia
[3] Chongqing Key Laboratory of Nanomaterials and Devices, Chongqing University of Science and Technology (CQUST), Chongqing, China
[4] Baykov Metallurgy and Materials Institute, Leninskii prosp., 49, 119334 Moscow, Russia
[5] Kosygin Russian State University, Malaya Kaluzhskaya 1, 119071, Moscow, Russia
[6] Department of Space Research, Lomonosov Moscow State University, Building, 3, Leninskie Gory, 1, 119991 Moscow, Russia
* Correspondence: safronovatv@my.msu.ru; Tel.: +7-(916)-3470641

Abstract: Powders with phase composition including syngenite $K_2Ca(SO_4)_2{\cdot}H_2O$ and/or calcium sulfate dihydrate (gypsum) $CaSO_4{\cdot}2H_2O$ were synthesized from powder of calcium carbonate $CaCO_3$ and water solutions of potassium hydrosulfate $KHSO_4$ of various (0.5M, 1M and 2M) concentrations. Molar ratio of starting salt $KHSO_4/CaCO_3=2$ were used to provide formation of syngenite $K_2Ca(SO_4)_2{\cdot}H_2O$. But when using 0.5M water solution of potassium hydrosulfate $KHSO_4$ the phase composition of synthesized powder was presented by calcium sulfate dihydrate (gypsum) $CaSO_4{\cdot}2H_2O$. When using 1M and 2M water solution of potassium hydrosulfate $KHSO_4$ the syngenite $K_2Ca(SO_4)_2{\cdot}H_2O$ was found as predominant phase in synthesized powders. According estimations made from thermal analysis data when 1.0M and 2.0M water solutions of potassium hydrosulfate $KHSO_4$ were used the content of calcium sulfate dihydrate (gypsum) $CaSO_4{\cdot}2H_2O$ in these powders were not higher then as 7.9 and 1.9 % respectively. Phase composition of products isolated from mother liquors via water evaporation consisted of syngenite $K_2Ca(SO_4)_2{\cdot}H_2O$ and potassium sulfate (arcanite) K_2SO_4. Synthesized powders can be used in preparation of biocompatible bioresorbable materials with phase composition in the K_2O-CaO-SO_3-H_2O system; as matrix of thermo- or photo-luminescent materials; as components reducing the setting time and increasing strength of sulfate cements; in the fertilizing industry and also as a components of Martian regolith simulant.

Keywords: potassium hydrosulfate; calcium carbonate; heterophase synthesis; syngenite; gypsum; arcanite

1. Introduction

The following mineral salts belong to the K_2O-CaO-SO_3-H_2O system: potassium sulfate K_2SO_4, potassium pyrosulfate $K_2S_2O_7$, potassium hydrosulfates $KHSO_4$, $K_3H(SO_4)_2$, $K_9H_7(SO_4)_8{\cdot}H_2O$, calcium sulfate hemihydrate $CaSO_4{\cdot}0.5H_2O$, calcium sulfate dihydrate $CaSO_4{\cdot}2H_2O$, syngenite $K_2Ca(SO_4)_2{\cdot}H_2O$, and gorgeyite $K_2SO_4{\cdot}5CaSO_4{\cdot}H_2O$ [1,2]. These minerals existing in different subsystems of K_2O-CaO-SO_3-H_2O system [3–7], especially syngenite $K_2Ca(SO_4)_2{\cdot}H_2O$, are important for several applications, among which are fertilizer industry [8,9], production of construction materials [10–12], inorganic materials with specific properties [13], creation of bioresorbable and biocompatible materials [14,15], creation of Martian regolith simulants [16–18].

Syngenite $K_2Ca(SO_4)_2{\cdot}H_2O$ can be synthesized using several different techniques: by crystallization at room temperature (20 °C and ~50% relative humidity) during evaporation of a solution containing calcium sulfate $CaSO_4$ and potassium sulfate K_2SO_4 in a molar ratio of 1:50 [19]; via interaction of hot solutions (80 °C, 100 °C) of calcium nitrate $Ca(NO_3)_2$ and potassium sulfate K_2SO_4 [20]; via interaction of calcium sulfate $CaSO_4$ and potassium chloride KCl in water medium [21]; or under mechanical activation in planetary mill from powder mixture of potassium sulfate K_2SO_4 and calcium sulfate dihydrate $CaSO_4{\cdot}2H_2O$ [17,22].

Syngenite $K_2Ca(SO_4)_2{\cdot}H_2O$ as a solid cement stone was synthesized by adding of water to the powder mixture consisting of calciolangbeinite $K_2Ca_2(SO_4)_3$ and potassium sulfate K_2SO_4 [15] or to the powder mixture of calcium sulfate $CaSO_4$ and potassium sulfate K_2SO_4 [23].

The aim of this investigation consisted in the development of robust method of synthesis of syngenite $K_2Ca(SO_4)_2{\cdot}H_2O$ powder not containing reaction by-products which need to be removed via washing of precipitate. Chemical interaction of powder of calcium carbonate $CaCO_3$ and potassium hydrosulfate $KHSO_4$ water solution will provide forming both target precipitate and unstable reaction by-product H_2CO_3 which can decompose during synthesis forming H_2O and CO_2. The release of gaseous CO_2 from the reaction zone will be an expected sign of a chemical reaction.

2. Materials and Methods

2.1. Materials

Powders of $CaCO_3$ (GOST 4530-76, Rushim, Moscow, Russia) and $KHSO_4$ (GOST 4223-75, Rushim, Moscow, Russia) were used for syntheses of powders.

2.2. Synthesis of Powders

Quantities of reagents were calculated according to Reaction (1).

$$2KHSO_4 + CaCO_3 = K_2Ca(SO_4)_2{\cdot}H_2O + CO_2, \qquad (1)$$

Molar ratio of starting salts $KHSO_4/CaCO_3$ in each synthesis was equal 2 and taken according to reaction (1) to produce syngenite $K_2Ca(SO_4)_2{\cdot}H_2O$. Table 1 contains labeling and synthesis conditions of powders under investigation. 400 ml of 0.5M, 1.0M, 2.0M $KHSO_4$ water solutions were prepared and used in the experiment. Calculated quantities of $CaCO_3$ power were added to each solution. Suspensions were kept on magnetic stirrer during 3 hours until the gas release stopped. Conditions of powders' synthesis and labeling of samples under investigation are presented in Table 1.

Table 1. Conditions of powders' synthesis. Labeling used for synthesized powders under investigation.

Labeling[1]	**Concentration of the $KHSO_4$ solution, mol/l**	**Volume of the solution, ml**	**The amount of substances by reaction, mol**		**Mass of reagents, g**		**Expected mass of $K_2Ca(SO_4)_2{\cdot}H_2O$, g**
			$KHSO_4$	**$CaCO_3$**	**$KHSO_4$**	**$CaCO_3$**	
SP0.5M	0.5	400	0.2	0.1	27.2	10.0	32.8
SP1.0M	1	400	0.4	0.2	54.4	20.0	65.6
SP2.0M	2	400	0.8	0.4	108.8	40.0	131.2

[1] SP – synthesized powder.

Precipitates were separate from the mother liquor using vacuum filtration, placed in the plastic trays and left to dry for a week. Then powders were collected, weighted, crushed in the agate mortar and passed through the sieve with the 200 μm cells. Transparent mother liquors were collected and products solved in were extracted from solutions via evaporation when keeping them at 40 °C for water evacuation and products crystallization. Substances extracted from mother liquors separated from synthesized powders SP0.5M SP1.0M and SP2.0M were labeled as Ex-SP0.5M, Ex-SP1.0M, Ex-SP2.0M respectively.

2.3. Methods of Analysis

The phase composition of the powders obtained after the synthesis and drying was determined by X-ray powder diffraction (XRD) analysis using Rigaku Miniflex 600 diffractometer (CuKα radiation, Kβ filter, and D/teX Ultra detector) in Bragg–Brentano geometry (Rigaku Corporation, Tokyo, Japan) with an angle interval 2Θ from 5° to 70° (step 2Θ – 0.02°). Phase analysis was performed using the ICDD PDF2 database [24] and Match software (version https://www.crystalimpact.com/, 15 August 2024).

Bulk densities of samples were calculated as mass of 1,0 ml of synthesized powders after drying, crashing in the agate mortar and passing through the sieve with 200 μm sells.

Scanning electron microscopy (SEM) images of the synthesized powder were characterized by SEM on Tescan Vega II (Tescan, Brno, Czech Republic) at accelerating voltages from 1 to 20 kV in secondary electron imaging mode (SE2 detector). Gold layers (≤10 nm in thickness) on the surface of the powder samples were applied (Quorum Technologies spraying plant, Q150T ES, Great Britain, London, UK).

Thermal analysis (TA) including thermogravimetry (TG) and differential thermal analysis (DTA) was performed using an NETZSCH STA 449 F3 Jupiter thermal analyzer (NETZSCH, Selb, Germany) during heating in air (10 °C/min, 40–1000 °C), the specimen mass being at least 10 mg. The gas-phase composition was monitored by a Netzsch QMS 403 Quadro quadrupole mass spectrometer (NETZSCH, Selb, Germany) coupled with a NETZSCH STA 449 F3 Jupiter thermal analyzer (NETZSCH, Selb, Germany). The mass spectra were registered for the following m/Z values: 18 (H_2O); 64 (SO_2).

3. Results and Discussion

According to the XRD data of synthesized powders shown in Figure 1, the phase composition of SP0.5M powder included $CaSO_4{\cdot}2H_2O$ (PDF card 33-313). The phase composition of SP1.0M and SP2.0M powders was represented preferably by syngenite $K_2Ca(SO_4)_2{\cdot}H_2O$ (PDF card 28-739) and $CaSO_4{\cdot}2H_2O$ in small extent. Reflexes of $CaSO_4{\cdot}2H_2O$ in XRD graph of SP2.0M powder hardly can be seen in the Figure 1 but in case of greater magnification very small reflexes could be seen. No traces of starting salts presented in the synthesized powders.

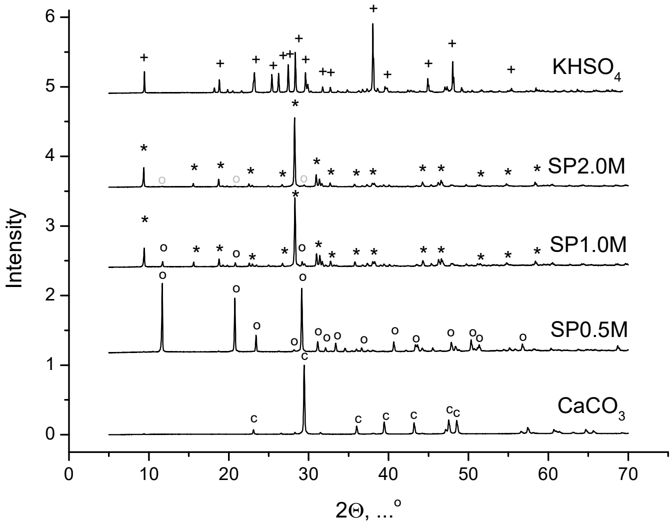

Figure 1. XRD of starting salts and synthesized powders: + - $KHSO_4$ (card PDF 11-649); * - $K_2Ca(SO_4)_2{\cdot}H_2O$ (card PDF 28-739); o - $CaSO_4{\cdot}2H_2O$ (card PDF 33-311); c – $CaCO_3$ (PDF card # 5-586).

Phase composition determined using Match software and mass of synthesized powders are summarized in Table 2.

Table 2. Phase composition and mass of synthesized powders.

Labeling	Expected mass of $K_2Ca(SO_4)_2{\cdot}H_2O$, g	Mass of synthesized powder, g	Phase composition of synthesized powder[1], mass %	
			$K_2Ca(SO_4)_2{\cdot}H_2O$ (#96-900-8129)[1]	$CaSO_4{\cdot}2H_2O$ (#96-901-7314)[1]
SP0.5M	32.8	15.5	0	100
SP1.0M	65.6	58.2	92.9	7.1
SP2.0M	131.2	114.3	98.7	1.3

[1] According to data obtained using Match software.

The calcium sulfate dihydrate $CaSO_4{\cdot}2H_2O$ present in the synthesized powder could be obtained according in accordance with the reaction (2).

$$2KHSO_4 + CaCO_3 + H_2O = CaSO_4{\cdot}2H_2O + CO_2 + K_2SO_4, \qquad (2)$$

Using Match software gypsum was determined in quantity of 7.1 and 1.3 mass % in powders SP1.0M and SP2.0M respectively. One can see that the syngenite $K_2Ca(SO_4)_2{\cdot}H_2O$ content in the synthesized powder depended on the conditions of the synthesis and increased with increasing of concentrations of the initial reagents (Table 2).

Camera photos of products extracted via evaporation from the transparent mother liquors are shown in Figure 2. There is no noticeable difference in the appearance of products collected from mother liquors except obviously bigger quantity of Ex-SP0.5M. All extracted products consisted of white transparent elongated crystals.

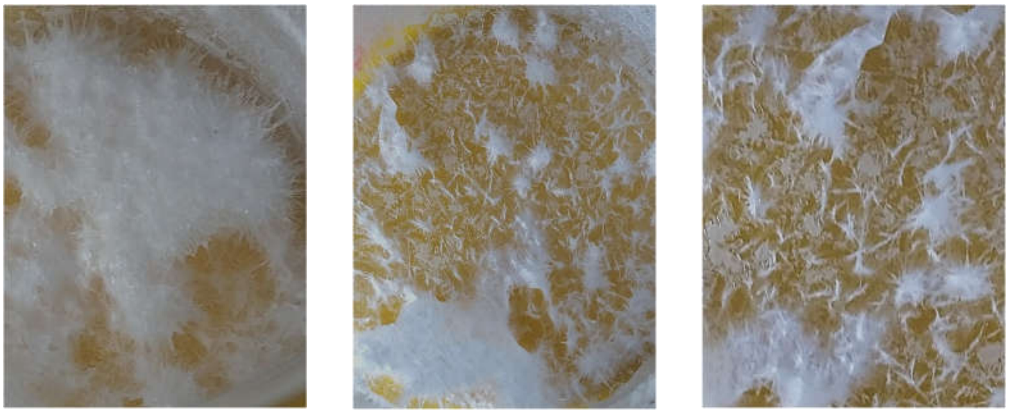
(**a**) (**b**) (**c**)

Figure 2. Camera photos of products extracted from mother liquors separated from precipitates via filtration and evaporation: Ex-SP0.5M (**a**), Ex-SP1.0M (**b**), Ex-SP2.0M (**c**).

According XRD the phase composition of products extracted via evaporation from the mother liquors (Figure 3) consisted of potassium sulfate (arcanite) K_2SO_4 (card PDF 5-613) and syngenite $K_2Ca(SO_4)_2{\cdot}H_2O$.

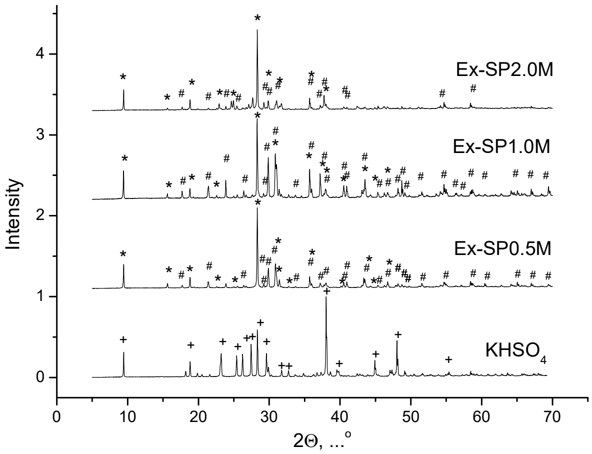

Figure 3. XRD of products extracted from mother solutions separated from precipitates after water evaporation and $KHSO_4$ given for comparison: * - $K_2Ca(SO_4)_2{\cdot}H_2O$ (card PDF 28-739); # - K_2SO_4 (card PDF 5-613); + - $KHSO_4$ (card PDF 11-649).

The presence of K_2SO_4 in the extracted products was provided due to reaction (2), and $K_2Ca(SO_4)_2{\cdot}H_2O$ (K_{sp} ($K_2Ca(SO_4)_2{\cdot}H_2O$) = 1.88 × 10^{-4}) formed due to presence of Ca^{2+}, K^+ and SO_4^{2-} in the mother liquors during water evaporation. The phase composition determined using Match software and mass the of extracted products are shown in Table 3. The higher the concentration of water solutions of potassium hydrosulfate $KHSO_4$ the lower the mass of products extracted from mother liquors and lower the contents of potassium sulfate K_2SO_4 in the extracted products are.

Table 3. Phase composition and mass of products extracted from mother liquors.

Labeling	**Mass of extracted product, g**	**Phase composition of extracted products[1], mass %**	
		$K_2Ca(SO_4)_2{\cdot}H_2O$ (#96-900-8129)[1]	K_2SO_4 (#96-900-7570)[1]
Ex-SP0.5M	17.21	62.2	37.8
Ex-SP1.0M	5.8	49.1	50.9
Ex-SP2.0M	5.6	83.3	16.7

[1] According to data from Match software.

SEM-images of synthesized powders are presented in Figure 4.

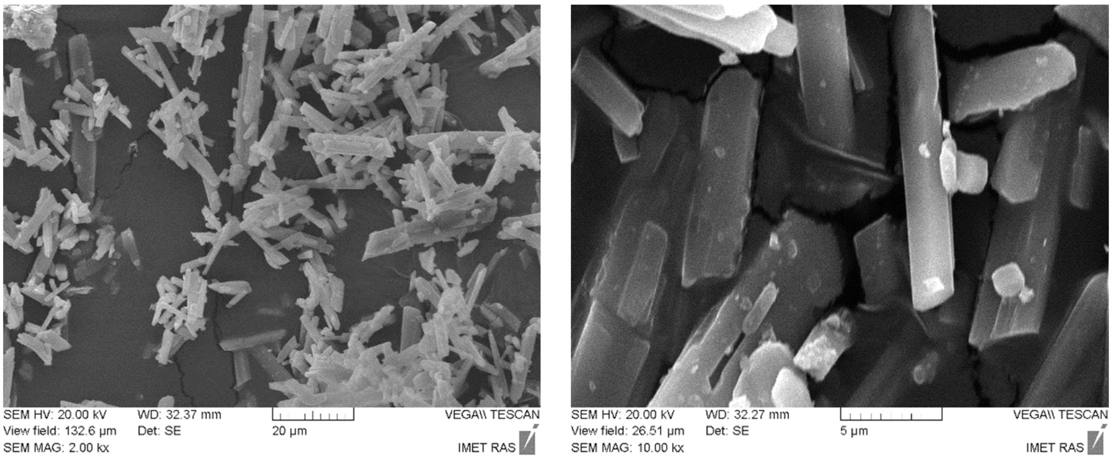

(**a**) (**b**)

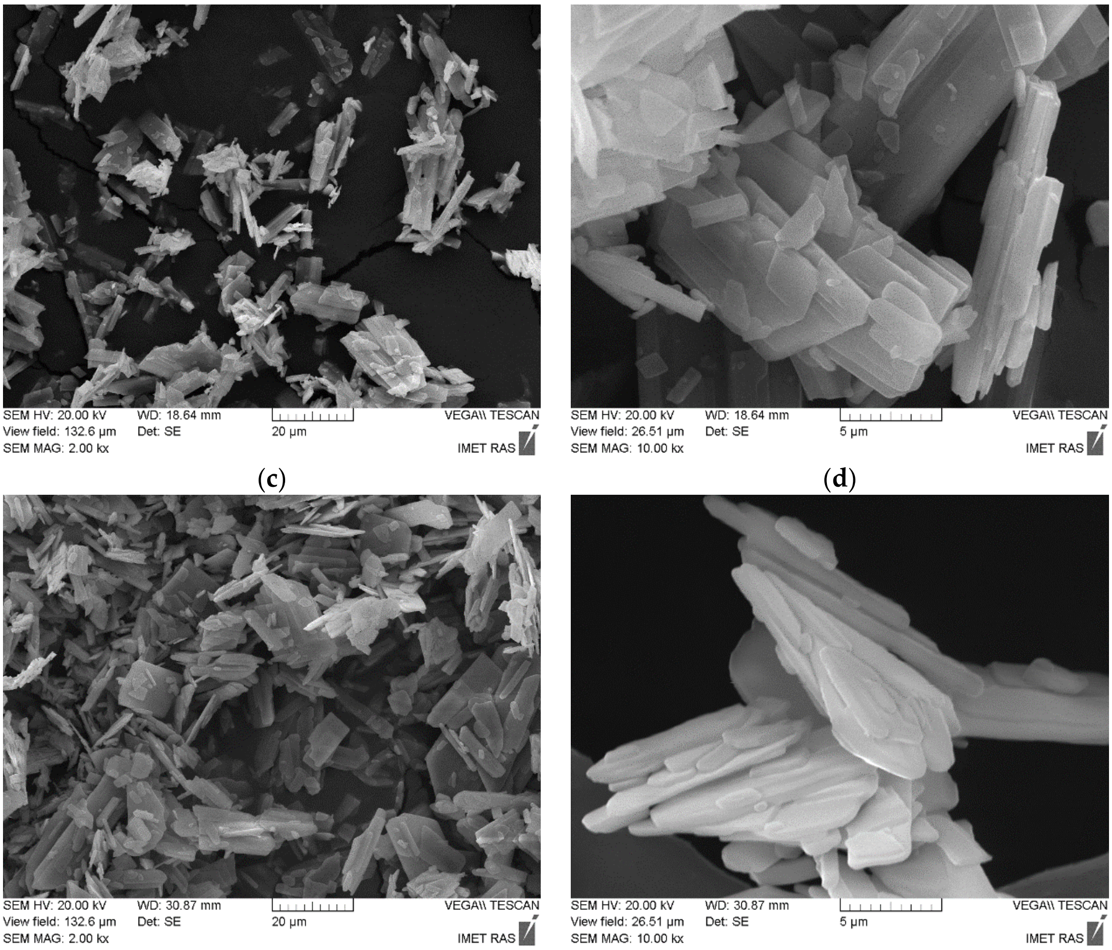

(**c**) (**d**)

(**e**) (**f**)

Figure 4. SEM images of the powders synthesized from powder of $CaCO_3$ and water solutions of $KHSO_4$ with concentration 0.5M (**a**,**b**); 1.0M (**c**,**d**); and 2.0M **(e**,**f**).

Powder SP0.5M with phase composition presented by gypsum $CaSO_4{\cdot}2H_2O$ consisted of particles having elongated prismatic morphology, which was typical for this mineral, with 5-20 µm long and 2-4 µm wide. Powders SP1.0M and SP2.0M with phase composition presented preferably by syngenite $K_2Ca(SO_4)_2{\cdot}H_2O$ consisted of particles having plate morphology which is typical for this mineral [15] with dimension 4-20 µm and 0.5-2 µm thick. It should be noted that syngenite $K_2Ca(SO_4)_2{\cdot}H_2O$ earlier was found to form elongated crystals [25] or even can also form "felt-like structure consisting of long, rail-like crystals" with a length of 10–20 µm in the paste based on the $CaSO_4{\cdot}2H_2O$ and K_2SO_4 [26].

Plate and elongated morphology of particles and their small dimensions can be taken as a reason of low balk density of synthesized powders which was 0.85, 0.80 and 0.86 g/cm^3 for powders SP0.5M, SP1.0M and SP2.0M respectively (Figure 5). Taking into account calculated density of gypsum $CaSO_4{\cdot}2H_2O$ (2.310 g/cm^3, # 96-901-7314, Match) and syngenite $K_2Ca(SO_4)_2{\cdot}H_2O$ (2.575 g/cm^3, # 96-900-8129, Match) relative densities of powders SP0.5M, SP1.0M and SP2.0M were 37, 34 and 33 % respectively.

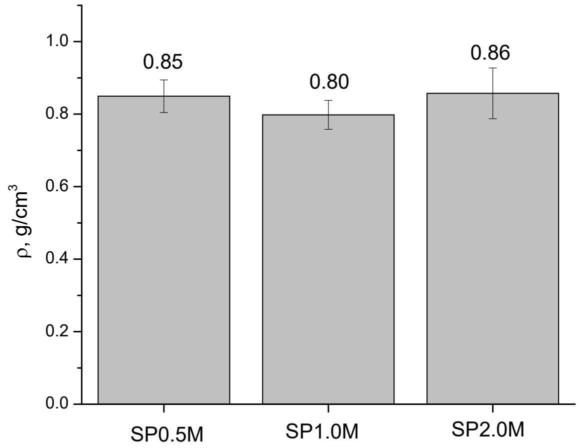

Figure 5. Bulk densities of synthesized powders.

Thermal analysis data for the synthesized powders are shown at Figure 6.

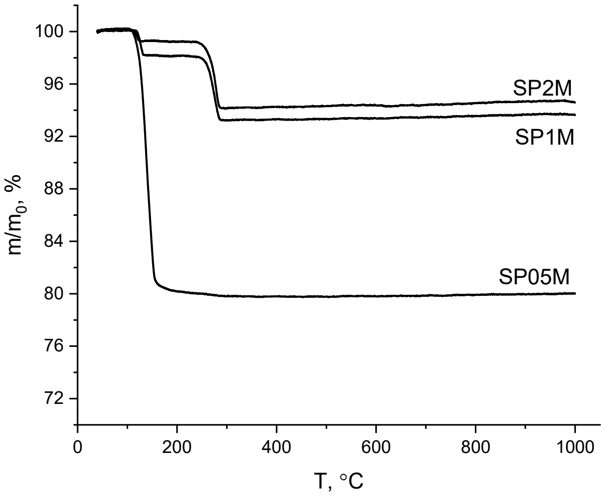

Figure 6. Thermal analysis data of the synthesized powders.

Total mass loss of powder SP0.5M at 1000 °C was 20.7% and this was in the good agreement with the possible mass loss of gypsum $CaSO_4{\cdot}2H_2O$ (20,9%) according to equation (2).

$$CaSO_4{\cdot}2H_2O = CaSO_4 + 2H_2O \quad (2)$$

Total mass loss of powders SP1.0M and SP2.0M were 6.7% and 5.7% at 1000 °C respectively. No traces of SO_2 (m/Z=64) were registered in the released gas phase during heating. Mass spectra for H_2O (m/Z=18) confirmed that mass loss of all synthesized powders during heating were due to H_2O evacuation (Figure 7). H_2O left sample SP0.5M in interval 90-200 with maximum at 144 °C. Mass loss of SP1.0M and SP2.0M went through two stage. First stage for powders SP1.0M were in the interval 106-155 °C with maximum at 134 °C and SP2.0M in the interval 99-153 °C with maximum 128 °C. This mass loss for powders SP1.0M and SP2.0M also could be due to decomposition of the smallest quantity of gypsum $CaSO_4{\cdot}2H_2O$ which were found by means of XRD (Figure 1, Table 2). Mass loss at the first stage of TA data give as opportunity to estimate quantity of gypsum $CaSO_4{\cdot}2H_2O$ as 7.9 and 1.9 % in powders SP1.0M and SP2.0M respectively. It worth to note that the estimation made taking into account TA data is close to the estimation of quantity of gypsum $CaSO_4{\cdot}2H_2O$ made by using Match software. The second stage of mass loss of SP1.0M and SP2.0M were in interval 230-310 °C with maximum 276 °C. This interval corresponds to the interval 250-300 °C determined previously [27]. Temperature interval 230-280 °C was used earlier for investigation of syngenite $K_2Ca(SO_4)_2{\cdot}H_2O$

decomposition in the isothermal conditions [28]. Taking into account XRD data reaction (3) could reflect the process of thermal decomposition of syngenite $K_2Ca(SO_4)_2{\cdot}H_2O$ in this interval.

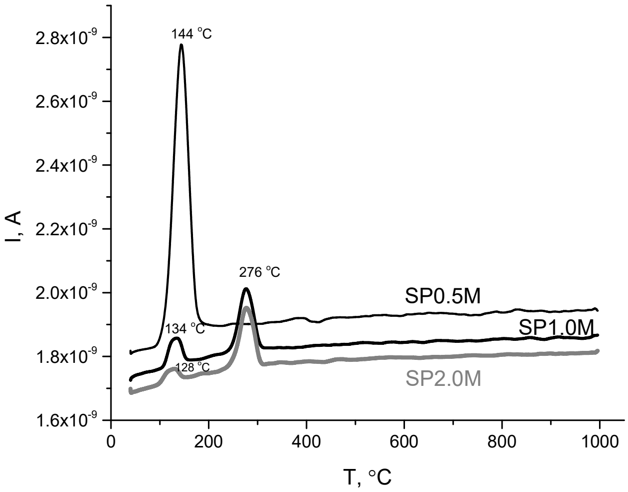

Figure 7. Mass spectra of the synthesized powders for m/Z=18.

$$K_2Ca(SO_4)_2{\cdot}H_2O = K_2Ca(SO_4)_2 + 2H_2O \qquad (3)$$

Endothermal effect for SP05M at interval 100-230 °C with minimum at 147 °C which was due to thermal dehydration of gypsum $CaSO_4{\cdot}2H_2O$ (Figure 8).

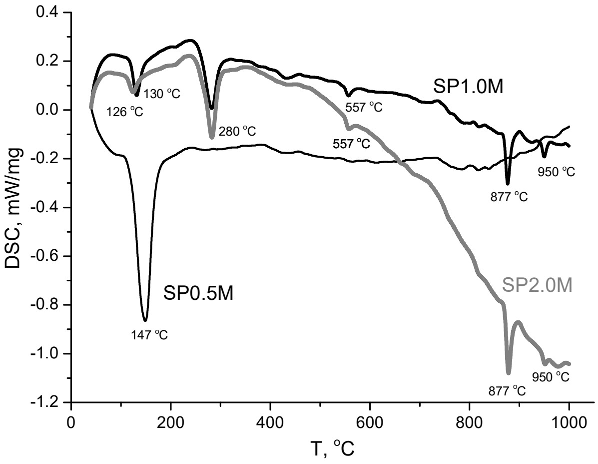

Figure 8. DSC of the synthesized powders.

There are 5 endothermal effects at the DSC curves of powders SP1.0M and SP2.0M. Endothermal effect in the intervals 90-180 °C with minimum at 130 °C (SP1.0M) and 90-160 °C with minimum at 126 °C (SP2.0M) correspond to thermal decomposition of gypsum $CaSO_4{\cdot}2H_2O$ presenting in these powders (reaction (2)). Endothermal effect in the interval 240-310 °C with minimum at 280 °C for powders SP1.0M and SP2.0M was due to dehydration of sygenite $K_2Ca(SO_4)_2{\cdot}H_2O$ (reaction (3)). The following three endothermal effects for SP1.0M and SP2.0M powders are at 557, 877 and 950 °C. According to the binary system K_2SO_4-$CaSO_4$ the following phases potassium sulfate K_2SO_4, calcium sulfate $CaSO_4$ and calciolangbeinite $K_2Ca_2(SO_4)_3$ exist in this system before 500 °C [29]. Reactions (4) and (5) can reflect formation of all these minerals [30,31].

$$3K_2Ca(SO_4)_2 \rightarrow K_2Ca_2(SO_4)_3 + 2K_2SO_4 + CaSO_4 \qquad (4)$$

$$2\ K_2Ca(SO_4)_2 \rightarrow K_2Ca_2(SO_4)_3 + K_2SO_4 \qquad (5)$$

There is transformation of β-K_2SO_4 to α-K_2SO_4 at 550 °C, formation of eutectic melt at 875 °C and transformation of $K_2Ca_2(SO_4)_3$ to $K_2Ca_2(SO_4)_3$ at 940 °C in the binary system K_2SO_4-$CaSO_4$. Endothermal effects at the experimental curves for SP1.0M and SP2.0M powders are in the obvious agreement with the events possible according with existing information about binary system K_2SO_4-$CaSO_4$.

4.. Conclusions

A new method for the powder synthesis with phase composition represented preferably by syngenite $K_2Ca(SO_4)_2{\cdot}H_2O$ from 1M and 2M water solutions of potassium hydrosulfate $KHSO_4$ and powder of calcium carbonate $CaCO_3$ as starting reagents has been proposed. By using of TA and XRD data it was found that content of calcium sulfate dihydrate (gypsum) $CaSO_4{\cdot}2H_2O$ in powders synthesized from 1M and 2M water solutions of potassium hydrosulfate $KHSO_4$ were not higher then as 7.9 and 1.9 % respectively. According SEM images these powders consisted of particles with plate morphology. When using 0.5M water solution of potassium hydrosulfate $KHSO_4$, powder of calcium sulfate dihydrate (gypsum) $CaSO_4{\cdot}2H_2O$ consisting of particles with elongated prismatic morphology was obtained. The phase composition of extracted products isolated from the mother liquors collected after all syntheses was represented by potassium sulfate K_2SO_4 and syngenite $K_2Ca(SO_4)_2{\cdot}H_2O$. Synthesized powders including precipitated and separated from mother liquors can be used in preparation of biocompatible bioresorbable materials with phase composition in the K_2O-CaO-SO_3-H_2O system, as matrixes of luminescent materials, as components reducing the setting time and increasing strength of sulfate cements, in the fertilizing industry and also as a component of Martian regolith simulant.

Author Contributions: Conceptualization, T.V.S.; methodology, T.V.S.; investigation, T.V.S., P.D.L., A.I.Z., X.L., T.B.S., O.V.B., D.R.K., M.M.A., Z.X. and M.R.A.; resources, D.R.K., T.B.S., O.V.B.; writing—original draft preparation, P.D.L., A.I.Z., T.V.S.; writing—review and editing, T.V.S.; visualization, T.V.S., P.D.L., A.I.Z., D.R.K., T.B.S., O.V.B., M.M.A. and M.R.A.; supervision, T.V.S.; project administration, T.V.S.; funding acquisition, M.R.A. All authors have read and agreed to the published version of the manuscript.

Funding: This work was carried out with the support of the MSU Program of Development, Project No 23-SCH01-16.

Acknowledgments: In this section, you can acknowledge any support given which is not covered by the author contribution or funding sections. This may include administrative and technical support, or donations in kind (e.g., materials used for experiments).

Conflicts of Interest: The authors declare no conflicts of interest.

References

1. Damidot, D., & Glasser, F. P. Thermodynamic investigation of the CaO-Al_2O_3-$CaSO_4$-K_2O-H_2O system at 25°C. *Cem. Concr. Res.*, **1993**, *23(5)*, 1195-1204. https://doi.org/10.1016/0008-8846(93)90180-H
2. Timakov, I. S., Grebenev, V. V., Komornikov, V. A., Zainullin, O. B., Makarova, I. P., Selezneva, E. V., & Kuzmin, I. I. Production of Complex Hydrosulphates in the $K_3H(SO_4)_2$–$Rb_3H(SO_4)_2$ Series: II. Phase Equilibria in the K_2SO_4–Rb_2SO_4–H_2SO_4–H_2O System. *Crystallogr. Rep.* **2022**, 67(3), 455-463. https://doi.org/10.1134/S106377452203021X
3. Eriksen, K. M., Fehrmann, R., Hatem, G. et al. Conductivity, NMR, Thermal Measurements, and Phase Diagram of the $K_2S_2O_7$–$KHSO_4$ System. The Journal of Physical Chemistry. **1996**, *100(25)*, 10771-10778. https://doi.org/10.1021/jp953744l
4. Komornikov, V.A., Timakov, I.S., Makarova, I.P., Selezneva, E.V., Grebenev, V.V., & Zainullin, O.B. (2020, December). The Study of Phase Equilibria and Superprotonic Crystals in the $(NH_4)_2SO_4$ - K_2SO_4 - H_2SO_4 - H_2O system. *J. Phys. Conf. Ser.* **2020** *1686 (1)*, 012048). IOP Publishing.https://doi.org/10.1088/1742-6596/1686/1/012048
5. Freyer, D., Voigt, W. Crystallization and phase stability of $CaSO_4$ and $CaSO_4$–based salts //Monatshefte für Chemie/Chemical Monthly. **2003**, *134(5)*, 693-719. https://doi.org/10.1007/s00706-003-0590-3
6. Safronova, T.V.; Belokozenko, M.A.; Yahyoev, S.O.; Shatalova, T.B.; Kazakova, G.K.; Peranidze, K.K.; Toshev, O.U.; Khasanova, S.S. Ceramics Based on $CaSO_4{\cdot}2H_2O$ Powder Synthesized from $Ca(NO_3)_2$ and $(NH_4)_2SO_4$. *Inorg. Mater.* **2021**, *57*, 867–873. https://doi.org/10.1134/S0020168521080112

7. Zhou, J.; Yuan, F.; Peng, S.; Xie, H.; Wu, P.; Feng, P.; Gao, C.; Yang, Y.; Guo, W.; Lai, D.; et al. Tunable Degradation Rate and Favorable Bioactivity of Porous Calcium Sulfate Scaffolds by Introducing Nano-Hydroxyapatite. *Appl. Sci.* **2016**, *6*, 411. https://doi.org/10.3390/app6120411
8. Mananda, A.B., Harada, H., Halem, H.I.A., Mitoma, Y., & Keiko, F. Study of potassium recovery from biomass ash using tartaric acid and syngenite method. *J. Mater. Scie. Chem. Eng.* **2021**, *9(5)*, 39-52. https://doi.org/10.4236/msce.2021.95004
9. Otani, T., Ando, H., Goshima, T., Mizuta, K., & Nii, S. Enhanced recovery of potassium from sugarcane molasses for fertilizer. *Sugar Tech*, **2023**, *25(4)*, 820-826. https://doi.org/10.1007/s12355-023-01248-1
10. Neto, J. D. S. A., Angeles, G., & Kirchheim, A. P. Effects of sulfates on the hydration of Portland cement–A review. *Constr. Build. Mater.* **2021**, *279*, 122428. https://doi.org/10.1016/j.conbuildmat.2021.122428
11. Arceo, H.B., Glasser, F.P. Fluxing reactions of sulphate and carbonates in cement clinkering. I. Systems $CaSO_4$-K_2SO_4 and K_2SO_4-$CaCO_3$. *Cem. Concr. Res.* **1990**, *20(6)*, 862-868. https://doi.org/10.1016/0008-8846(90)90047-2
12. Schiefer, C., & Plank, J. Mechanochemical syngenite as hydration accelerator for anhydrite-based self-levelling floor screeds. *Constr. Build. Mater.*, **2021**, *308*, 124982. https://doi.org/10.1016/j.conbuildmat.2021.124982
13. Pandey, A., Sonkawade, R.G., Sahare, P.D. Thermoluminescence and photoluminescence characteristics of nanocrystalline $K_2Ca_2(SO_4)_3$:Eu. *J. Phys. D.* **2002**, *35(21)*, 2744. https://doi.org/10.1088/0022-3727/35/21/309
14. Safronova, T.V.; Akhmedov, M.M.; Shatalova, T.B.; Tikhonova, S.A.; Kazakova, G.K. Ceramics in the K_2O–CaO–SO_3–P_2O_5 System. *Russ. J. Inorg. Chem.* **2021**, *66*, 1057–1066. https://doi.org/10.1134/S0036023621080246
15. Kuznetsov, A.I.; Safronova, T.V.; Shatalova, T.B.; Filippov, Y.Y.; Vaymugin, L.A.; Vlasenko, V.S.; Likhanov, M.S. Materials in the CaO-K_2O-SO_3-H_2O System Based on Powder Mixtures including Calciolangbeinite $K_2Ca_2(SO_4)_3$ and Calcium Sulfate Anhydrite $CaSO_4$. *Ceramics* **2023**, *6*, 1434-1448. https://doi.org/10.3390/ceramics6030088
16. García-Florentino, C., Gomez-Nubla, L., Huidobro, J., Torre-Fdez, I., Ruíz-Galende, P., Aramendia, J., ... & Madariaga, J.M. Interrelationships in the gypsum–syngenite–görgeyite system and their possible formation on mars. *Astrobiology*, **2021**, *21(3)*, 332-344. https://doi.org/10.1089/ast.2020.2319
17. Huidobro, J., Aramendia, J., Arana, G., Hausrath, E. M., & Madariaga, J. M. The effect of low temperature on the Raman spectra of calcium-rich sulfates on Mars. *Annals of Glaciology*. **2023**, *64*(91), 57-62. https://doi.org/10.1017/aog.2023.29
18. Ju, E., Shi, E., Xin, Y., Cao, H., Liu, C., Liu, P., ... & Ling, Z. Laboratory synthesis, spectroscopic characteristics, and conversion relationships of five calcium sulfate double salts relevant to Mars. *Icarus*. **2023**. *401*, 115610. https://doi.org/10.1016/j.icarus.2023.115610
19. Jentzsch, P.V., Bolanz, R.M., Ciobotă, V., Kampe, B., Rösch, P., Majzlan, J., & Popp, J. Raman spectroscopic study of calcium mixed salts of atmospheric importance. *Vib. Spectrosc.* **2012**, *61*, 206-213. http://dx.doi.org/10.1016/j.vibspec.2012.03.007
20. Jurišová, J. et al., Phase diagram of the system $CaSO_4$-K_2SO_4-KNO_3-$Ca(NO_3)_2$-H_2O. *Acta Chim. Slov.* **2014**, *7 (1)*, 20—24, http://dx.doi.org/10.2478/acs-2014-0004
21. Goncharik, I.I., Shauchuk, V.V., Kudzina, O.A., & Mozheyko, F.F. Preparation of potassium sulfate in a reaction of potassium chloride and calcium sulfate. *Proceedings of the National Academy of Sciences of Belarus, Chemical Series*. **2017**, *(3)*, 98-103. (In Russian) https://vestichem.belnauka.by/jour/article/view/276
22. Schiefer, C., & Plank, J. Solventless Mechanochemical Synthesis of Phase Pure Syngenite. *Chemistry-Methods*, **2021**, *1(1)*, 78-84. http://dx.doi.org/10.1002/cmtd.20200006483
23. Smillie, S.; Moulin, E.; Macphee, D.E.; Glasser, F.P. Freshness of cement: Conditions for syngenite $CaK_2(SO_4)_2$ H_2O formation. *Adv. Cem. Res.* **1993**, *19*, 93–96. https://doi.org/10.1680/adcr.1993.5.19.93
24. ICDD (2010). PDF-4+ 2010 (Database), edited by Dr. Soorya Kabekkodu, International Centre for Diffraction Data. Newtown Square. PA. USA. http://www.icdd.com/products/pdf2.htm
25. Matović, V., Erić, S., Kremenović, A., Colomban, P., Srećković-Batoćanin, D., & Matović, N. The origin of syngenite in black crusts on the limestone monument King's Gate (Belgrade Fortress, Serbia)–the role of agriculture fertiliser. *Journal of Cultural Heritage*, **2012,** *13(2)*, 175-186. https://doi.org/10.1016/j.culher.2011.09.003
26. Sanytsky, M., Kropyvnytska, T., & Shyiko, O. Effect of Potassium Sulfate on the Portland Cement Pastes Setting Behavior. *Chem. Chem. Technol.* **2023**, *17(1)*, 170-178. https://doi.org/10.23939/chcht17.01.170
27. Wieczorek-Ciurowa, K. Topochemistry of thermal dehydration of syngenite $K_2Ca(SO_4)_2{\cdot}H_2O$. *Thermochimica acta*, **1985**, *92*, 485-487. https://doi.org/10.1016/0040-6031(85)85921-9
28. Dankiewicz, J., & Wieczorek-Ciurowa, K. Kinetic study of the thermal dehydration of syngenite $K_2Ca(SO_4)_2H_2O$ under isothermal conditions. *J. Therm. Anal. Calorim.* **1978,** *13(3)*, 543-552. https://doi.org/10.1007/bf01912393
29. Rowe, J.J., Morey, G.W., & Hansen, I.D. The binary system K_2SO_4-$CaSO_4$. *J. Inorg. Nucl. Chem.* **1965**. *27(1)*, 53-58. https://doi.org/10.1016/0022-1902(65)80189-0

30. Kloprogge, J.T., Ding, Z., Martens, W.N., Schuiling, R.D., Duong, L.V., & Frost, R.L. Thermal decomposition of syngenite, $K_2Ca(SO_4)_2 \cdot H_2O$. *Thermochimica Acta*, **2004.** *417(1),* 143-155. https://doi.org/10.1016/j.tca.2003.12.001
31. Pekov I.V., Zelenski M.E., Zubkova N.V. et al. Calciolangbeinite, $K_2Ca_2(SO_4)_3$, a new mineral from the Tolbachik volcano, Kamchatka, Russia. *Mineralogical Magazine*. **2012,** *76(3),* 673-682. https://doi.org/10.1180/minmag.2012.076.3.16